

New Insights into the Catalytic Cycle of Flavocytochrome b_2 [†]

Simon Daff,[‡] W. John Ingledew,[§] Graeme A. Reid,^{||} and Stephen K. Chapman^{*,‡}

Department of Chemistry and Institute of Cell and Molecular Biology, University of Edinburgh, King's Buildings, West Mains Road, Edinburgh, Scotland, U.K., and School of Biological & Medical Sciences, University of St. Andrews, St. Andrews, Fife, Scotland, U.K.

Received September 20, 1995; Revised Manuscript Received January 16, 1996[®]

ABSTRACT: Flavocytochrome b_2 from *Saccharomyces cerevisiae* couples L-lactate dehydrogenation to cytochrome c reduction in the mitochondrial intermembrane space. The catalytic cycle for this process can be described in terms of five consecutive electron-transfer events. L-Lactate dehydrogenation results in the two-electron reduction of FMN. The two electrons are individually passed to b_2 -heme (intramolecular electron transfer) and then onto cytochrome c (intermolecular electron transfer). At 25 °C, I 0.10, in the presence of saturating concentrations of ferricytochrome c and L-lactate, the catalytic cycle progresses with rate constant $104 (\pm 5) \text{ s}^{-1}$ [per L-lactate oxidized; Miles, C. S., Rouviere-Fourmy, N., Lederer, F., Mathews, F. S., Reid, G. A., & Chapman, S. K. (1992) *Biochem. J.* 285, 187–192]. Stopped-flow spectrophotometry has been used to show that the major rate-limiting step in the catalytic cycle is electron transfer from flavin semiquinone to b_2 -heme. This conclusion is based on the observation that pre-steady-state flavin oxidation by ferricytochrome c takes place at 120 s^{-1} . Although flavin oxidation involves several other electron transfer steps, these are considered too fast to contribute significantly to the rate constant. It was also shown that the reaction product, pyruvate, is able to inhibit pre-steady-state flavin oxidation ($K_i = 40 \pm 17 \text{ mM}$) consistent with reports that it acts as a noncompetitive inhibitor in the steady state at high concentrations [$K_i = 30 \text{ mM}$; Lederer, F. (1978) *Eur. J. Biochem.* 88, 425–431]. This novel way of measuring the electron transfer rate constant is directly applicable to the catalytic cycle and has enabled us to derive a self-consistent model for it, based also on data collected for enzyme reduction [Miles, C. S., Rouviere-Fourmy, N., Lederer, F., Mathews, F. S., Reid, G. A., & Chapman, S. K. (1992) *Biochem. J.* 285, 187–192] and its interaction with cytochrome c [Daff, S., Sharp, R. E., Short, D. M., Bell, C., White, P., Manson, F. D. C., Reid, G. A., & Chapman, S. K. (1996) *Biochemistry* 35, 6351–6357]. Rapid-freezing quenched-flow EPR has been used to confirm the model by demonstrating that during steady-state turnover of the enzyme approximately 75% of the flavin is in the semiquinone oxidation state.

Flavocytochrome b_2 from *Saccharomyces cerevisiae* is a soluble L-lactate cytochrome c oxidoreductase found in the mitochondrial intermembrane space (Daum et al., 1982). It is a homotetramer, with each 511 amino acid subunit consisting of two distinct domains. The first 100 residues fold to form a heme binding domain which is connected via a short hinge region to a flavin mononucleotide (FMN) binding domain. Finally, a 20 amino acid C-terminal tail winds around the 4-fold axis of the tetramer forming several interactions with each of the other subunits. The X-ray crystal structure, solved to 2.4 Å resolution (Xia & Mathews, 1990), identifies the site for L-lactate dehydrogenation which is constructed around the FMN prosthetic group. The two electrons generated by L-lactate dehydrogenation are used to reduce FMN to its hydroquinone form. They are then individually passed to two ferricytochrome c molecules via the b_2 -heme. Direct flavin to cytochrome c electron transfer

is negligible (Forestier & Baudras, 1971; Iwatsubo et al., 1977; Balme et al., 1995). The rate constant for enzyme turnover under the saturating conditions of 10 mM L-lactate and excess cytochrome c is $104 (\pm 5) \text{ s}^{-1}$ per mol of lactate per mol of enzyme (which is equivalent to $207 (\pm 10) \text{ s}^{-1}$ per mol of cytochrome c reduced), whereas the rate constant for the flavin reduction/lactate oxidation process is $604 (\pm 60) \text{ s}^{-1}$ (Miles et al., 1992). The latter value is subject to a ^2H kinetic isotope effect of $8.1 (\pm 1.4)$, whereas in the cycle as a whole this has been eroded to $3.0 (\pm 0.6)$. Clearly there is a slower step in the cycle which limits the enzyme's turnover rate. The catalytic cycle can be represented by a series of five consecutive electron-transfer steps which form the basis of the model described in Figure 1. Following FMN reduction/L-lactate oxidation (step 1) there are two FMN to b_2 -heme intramolecular electron transfers (steps 2 and 4), and two b_2 -heme to cytochrome c electron transfers (steps 3 and 5). The cytochrome c reduction steps are considered in detail by Daff et al. (1996) with the conclusion that the effect of these steps on the overall rate of the cycle is minimal. Intramolecular electron transfer from FMN hydroquinone to b_2 -heme (step 2) has been studied extensively by using stopped-flow spectrophotometry to monitor b_2 -heme reduction (Capeillère-Blandin, 1975; Capeillère-Blandin et al., 1975; Pompon et al., 1980; Pompon, 1980;

* To whom correspondence should be addressed. Fax: (44)131 650 4743. Email: S.K.Chapman@ed.ac.uk.

[†] This work was funded by the Biotechnology and Biological Science Research Council (U.K.), by The European Commission (FLAPS Network) and via a studentship from the Engineering and Physical Sciences Research Council (U. K.) to S.D.

[‡] Department of Chemistry, University of Edinburgh.

[§] University of St. Andrews.

^{||} Institute of Cell and Molecular Biology, University of Edinburgh.

[®] Abstract published in *Advance ACS Abstracts*, May 1, 1996.

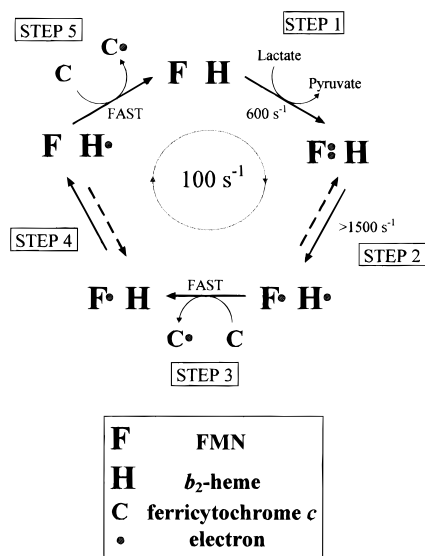


FIGURE 1: Model proposed to explain the catalytic cycle of flavocytochrome *b*₂ based on individual electron-transfer processes. The action of a single subunit of the enzyme is described as it turns over at its maximum rate of $\sim 100 \text{ s}^{-1}$ in the presence of saturating amounts of L-lactate and ferricytochrome *c* at 25 °C in 10 mM Tris-HCl buffer, pH 7.5, *I* 0.10. Two equivalents of cytochrome *c* are reduced in each turnover so in these terms the k_{cat} is 207 (± 10) s^{-1} (Miles et al., 1992). (Step 1) Reduction of FMN to its hydroquinone form, and oxidation of L-lactate to pyruvate. (Step 2) Interdomain electron transfer from fully reduced FMN to *b*₂-heme, generating reduced heme and FMN semiquinone. (Steps 3 and 5) Binding and reduction of ferricytochrome *c* by *b*₂-heme. (Step 4) Interdomain electron transfer from FMN semiquinone to *b*₂-heme.

Chapman et al., 1994), laser flash photolysis to monitor *b*₂-heme re-reduction (Hazzard et al., 1994), and site-directed mutagenesis to investigate the importance of the protein framework (Miles et al., 1992; Sharp et al., 1994; White et al., 1993). All of these experiments confirm that step 2 is several times faster than catalytic turnover, and, under our particular conditions, the rate constant is likely to be in excess of 1500 s^{-1} (Chapman et al., 1994). The second intramolecular electron transfer (step 4), which occurs from FMN semiquinone to *b*₂-heme, is less well understood but has been studied recently using laser flash photolysis (Walker & Tollin, 1991). However, electron transfer was only observed in the presence of pyruvate and in the reverse direction. Pyruvate is known to cause complex inhibition during the steady-state turnover of flavocytochrome *b*₂ (Lederer, 1978) and is able to stabilize the semiquinone redox state of FMN in both the *S. cerevisiae* (Walker & Tollin, 1991) and related *Hansenula anomala* enzymes (Tegoni et al., 1986, 1990).

In the present paper we describe how the use of stopped-flow spectrophotometry to study FMN oxidation in the presence of excess ferricytochrome *c* has enabled step 4 of the catalytic cycle to be monitored in the pre-steady-state, both in the absence and presence of pyruvate. The evidence obtained suggests that FMN semiquinone to *b*₂-heme electron transfer is the major rate-limiting step in the catalytic cycle, and that pyruvate inhibits this process. This has allowed a self-consistent kinetic model to be derived for the catalytic cycle (Figure 1) based on the electron transfers occurring when the enzyme is turning over in the presence of saturating concentrations of its physiological substrates. Confirmatory evidence for the model has been obtained from rapid-freezing quenched-flow EPR spectrometry which has enabled free-

radical quantities to be calculated for reaction mixtures frozen while in steady-state turnover.

MATERIALS AND METHODS

Enzyme Preparations. Flavocytochrome *b*₂ expressed in *Escherichia coli* was isolated from cells stored temporarily at -20°C using a previously reported purification procedure (Black et al., 1989). Purified enzyme samples were stored in the short term under nitrogen at 4°C as precipitates from 70% saturated $(\text{NH}_4)_2\text{SO}_4$ solution. Alternatively, long term storage was secured by snap-freezing drops of enzyme in liquid nitrogen and maintaining these at below -180°C . Before freezing, the enzyme was desalted using a Sephadex G25 gel filtration column (1.5 cm \times 15 cm) (Sigma) equilibrated and eluted with 10 mM Tris-HCl buffer, pH 7.5, *I* 0.10. The buffer consisted of 10 mM HCl titrated against Tris solution to pH 7.5 and adjusted to *I* 0.10 by addition of NaCl. All enzyme solutions used for kinetic analysis were found to have $>90\%$ activity based on the maximum steady-state rate of 400 s^{-1} (Miles et al., 1992) measured in the presence of 1 mM ferricyanide (potassium salt, BDH) and 10 mM L-lactate (Sigma). Enzyme concentrations were calculated using previously published extinction coefficients (Pajot & Groudinsky, 1970).

Stopped-Flow Kinetics. All stopped-flow experiments were carried out in 10 mM Tris, HCl buffer, *I* 0.10 at $25.0 (\pm 0.1)^\circ\text{C}$, using an Applied Photophysics SF.17 MV stopped-flow spectrofluorimeter, as described previously (Miles et al., 1992), analysis of kinetic data was performed using the SF.17 MV software and Origin (Microcal), both of which use nonlinear least-squares regression analysis. FMN and *b*₂-heme reduction were monitored as described previously (Miles et al., 1992) by following absorbance changes at 438.3 and 557 nm, respectively; in addition, pyruvate was introduced into the syringe containing L-lactate to ascertain its effect on these processes. The re-reduction of *b*₂-heme by flavin, following rapid oxidation by horse-heart cytochrome *c* (Sigma), was monitored at 408.4 nm, an isosbestic point in the cytochrome *c* spectrum. For this experiment 40 μM flavocytochrome *b*₂ reduced by 10 mM L-lactate was used in conjunction with 4 μM cytochrome *c*. Absorbance is then converted to percent *b*₂-heme oxidized, based on the quantity of cytochrome *c* used (4 μM), and the standard absorbance change for deflavoflavocytochrome *b*₂ calculated from an oxidized/reduced difference spectrum to be $44\,000 (\pm 5000) \text{ M}^{-1} \text{ s}^{-1}$.

FMN oxidation by an excess of cytochrome *c*, as illustrated in Figure 4, was monitored at the *b*₂-heme isosbestic wavelength of 438.3 nm, where standard absorption coefficients for the various redox states have been previously determined to be approximately 1200, 3000, and $10\,000 \text{ M}^{-1} \text{ cm}^{-1}$ for reduced, semiquinone, and oxidized, respectively (Capeillère-Blandin, 1991). Flavocytochrome *b*₂ was initially reduced by 1 mM glycolate (Sigma), a poor substrate with maximum turnover rate of $3.5 \text{ mol of substrate s}^{-1}$, in order to prevent rapid re-reduction of the enzyme. Since 438.3 nm is not an isosbestic for cytochrome *c*, its absorbance contribution at this wavelength had to be subtracted. This was achieved by generating a cytochrome *c* reduction trace at the *b*₂-heme/FMN isosbestic of 544.8 nm (Figure 3) (Janot et al., 1990). A pure FMN trace could be produced according to $\text{Absorbance}(438.3 \text{ nm}) + 107\%[\text{Absorbance}(544.8 \text{ nm})]$. The traces were collected using a split time-base, and the period of slow turnover, dependent on glycolate oxidation,

was used to determine the addition percentage used above. During a true steady-state period the absorbance of the FMN will be constant, and therefore the modified trace should be flat. In addition, once all the cytochrome c has reacted, the enzyme is reduced by the excess of glycolate and should therefore return to its original absorbance. Bearing these facts in mind, the value was derived by inspection. The error in this method, although difficult to quantify, can be expected to be less than 5%. Once modified, the fast phase of each trace, representing the time course for flavin oxidation and occurring largely within the first 100 ms, was fitted to a single-exponential function. The effect of the addition error on these rate constants is estimated to be less than 10%.

Inhibition of FMN oxidation by pyruvate (Sigma) was studied by introducing a range of different concentrations (0–50 mM) via the cytochrome c syringe. The kinetic analysis was then carried out as described above.

Quenched-Flow EPR Kinetics. The rapid quenched-flow EPR experiment was performed in 10 mM MOPS (morpholinopropanesulfonic acid, Sigma)/KOH buffer, pH 7.5, adjusted to I 0.10 by addition of NaCl. For each experimental data point, 1 mL of reaction mixture containing 470 μ M oxidized cytochrome c , 20 μ M flavocytochrome b_2 , and 10 mM L-lactate was generated by a rapid mixer and forced through a variable length of HPLC steel tubing before being sprayed into a bath of isopentane (Probalo), maintained at -140 °C by a liquid nitrogen cooled cryostat (Moodie et al., 1990). In order to vary the time-base for the experiment, different lengths of steel tube were used, to allow different degrees of aging. The frozen reaction mixture was then packed into an EPR tube and stored in liquid nitrogen. All EPR measurements were performed on a Bruker instrument. Integrals were calculated for the FMN semiquinone signal at -184 °C relative to a 1 mM Cu^{II} standard, and for the ferricytochrome c signal at -270 °C relative to a 1 mM ferricytochrome c standard. These were corrected for packing with respect to a standard ferricytochrome c sample produced in an identical way but in the absence of flavocytochrome b_2 . The ferricytochrome c integrals were used to calibrate the time base for the data in Figure 6 by fixing them to a spectrophotometrically collected cytochrome c trace which had been adjusted to account for the higher concentration of flavocytochrome b_2 and faster reaction rate observed in the quenched-flow experiment.

RESULTS AND DISCUSSION

The catalytic cycle for flavocytochrome b_2 is illustrated in Figure 1 in terms of its component electron transfer processes. This provides a convenient frame of reference for experiment since each electron transfer corresponds to a change in the visible absorption spectrum. It is important to note, however, that the rate determining factor in each electron transfer step may be dependent on a chemical or conformational change directly preceding the electron transfer, such that the observed color changes serve only as convenient observation points.

Step 1. FMN reduction by L-lactate has been studied previously using stopped-flow spectrophotometry (Miles et al., 1992). The rate constant for this process is reported as $604 (\pm 60) \text{ s}^{-1}$ with a ^2H kinetic isotope effect of $8.1 (\pm 1.4)$ on $\alpha\text{-H}$ abstraction. This step is 6-fold faster than the overall turnover rate, and for this reason it should contribute little toward rate limitation.

Step 2. b_2 -Heme reduction has been studied in tandem with FMN reduction and appears to lag behind by only a small amount. This suggests that the rate constant for electron transfer from FMN to b_2 -heme is faster than for FMN reduction. A conservative estimate of the rate constant for the electron-transfer process has been given as $1500 (\pm 500) \text{ s}^{-1}$ (Chapman et al., 1994) by considering the magnitude of the lag phase. However, accuracy is limited by the stopped-flow procedure which cannot generate reliable data for reactions which occur at this velocity and faster. Laser flash photolysis has also been used to study this electron-transfer process, providing a value for the rate constant of 1900 s^{-1} (Hazzard et al., 1994) at 24 °C in pH 7, 100 mM phosphate buffer, which is in agreement with the stopped-flow observations.

If pre-steady-state rate constants are to be applied directly to a steady-state situation, it is important to match the conditions as closely as possible. In the b_2 -heme reduction experiment described above, intramolecular electron transfer is only observed after FMN reduction and, in this respect, mimics step 1 and step 2 of the catalytic cycle. However, one factor missing from this experiment is the presence of cytochrome c which may bind strongly to the enzyme and affect either step. For this reason b_2 -heme reduction was carried out in the presence of zinc-substituted cytochrome c , a redox inactive form of the electron acceptor known to bind to flavocytochrome b_2 . The results are presented by Daff et al. (1996) and show that the stopped-flow traces overlay almost exactly, demonstrating that the binding of cytochrome c to flavocytochrome b_2 is unlikely to affect either step 1 or step 2.

In order to study FMN to b_2 -heme electron transfer in the presence of redox-active cytochrome c , the rapid b_2 -heme to cytochrome c electron-transfer process was exploited. This intermolecular step is dependent on the concentration of enzyme, and at high concentration ($>25 \mu\text{M}$) is known to occur within the dead-time of a stopped-flow experiment (Daff et al., 1996). By inducing the FMN to b_2 -heme electron transfer in fully reduced enzyme using a substoichiometric amount of cytochrome c to first partially oxidize the b_2 -heme, a " b_2 -heme re-reduction" trace is generated. The absorbance change observed gives the percent of oxidized b_2 -heme relative to the amount of ferricytochrome c used. The proportion of oxidized b_2 -heme reaches a maximum of 20–30%, meaning that electron transfer from the fully reduced FMN to b_2 -heme is happening too fast to be observed by this method; i.e., the rate constant must be in excess of 1000 s^{-1} . Some oxidized heme is observed because electron transfer from the fully reduced FMN to oxidized b_2 -heme will initially result in an equilibrium being established between the two prosthetic groups, based on their electrode potentials (Capeillère-Blandin, 1975; Chapman et al., 1994). This equilibrium is eventually disrupted by disproportionation of flavin semiquinones followed by reduction by L-lactate. This is an overall slower process than the initial electron transfer but leads to fully reduced enzyme which accommodates three electrons (i.e., back to the starting absorbance). This experiment was repeated using different substrates at different concentrations to reduce the enzyme, but in each case the maximum absorbance observed was never significantly different from that described above. In these experiments it is very unlikely that substrate (e.g., L-lactate) is bound in the active site when the enzyme is fully reduced (Urban et al., 1983), especially at low substrate

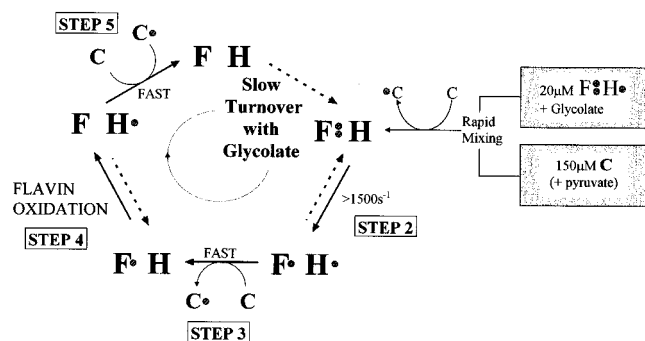


FIGURE 2: Electron-transfer processes occurring during the flavin oxidation stopped-flow experiment (see Materials and Methods). An excess of ferricytochrome *c* is used to oxidize flavocytochrome *b*₂ by entering the catalytic cycle (see Figure 1) immediately before step 2. The use of glycolate as substrate enables the enzyme to be fully reduced initially but dramatically slows down the overall turnover rate at step 1 (see Figure 1). This allows step 4, FMN oxidation, to be monitored as a pre-steady-state process. Examples of the stopped-flow traces derived from this experiment are illustrated in Figures 3 and 4. The introduction of pyruvate into the ferricytochrome *c* solution before mixing allows inhibition to be studied in the pre-steady-state.

concentrations. Further, since the product (e.g., pyruvate) is present only in a slight excess over the enzyme, this is also unlikely to be bound. Therefore, rapid FMN to *b*₂-heme electron transfer must be possible when the active site of the enzyme is empty. This observation is therefore complementary to the *b*₂-heme reduction experiment, which demonstrates that rapid electron transfer occurs directly after FMN reduction by L-lactate. In this case it is possible that pyruvate is still bound in the active site during the electron-transfer event. Therefore, we can conclude either that the presence of pyruvate has little effect on this electron-transfer step in terms of the catalytic cycle or that pyruvate dissociation is too fast to cause a detectable change in the rate.

In summary, there is no evidence to show that there is any significant impediment to the electron transfer from fully reduced FMN to *b*₂-heme that would contribute to limiting the overall turnover rate to 100 s⁻¹.

Steps 3 and 5. Both these steps represent electron transfers from the *b*₂-heme to cytochrome *c* but also involve binding and dissociation processes. These are discussed in detail in Daff et al. (1996) which concludes that the effects on the catalytic cycle are negligible.

Step 4. Flavin oxidation traces were collected as described in Materials and Methods (see Figures 2–4). By using the poor substrate, glycolate, to pre-reduce a solution of enzyme (20 μM before mixing) and mixing with an excess of ferricytochrome *c* (150 μM before mixing), step 4 of the cycle could be studied with the assurance that step 1, flavin reduction, would be slowed down enough to effectively rate-limit enzyme turnover. As already discussed, steps 2 and 3 occur too fast to be detected by stopped-flow spectrophotometry, and therefore the change observed with regard to FMN absorbance at 438.3 nm is limited to the conversion of the semiquinone to oxidized FMN. The cytochrome *c* trace monitored at 544.8 nm gives an overall indication of the processes occurring. The fast phase (first 100 ms) corresponds to a large absorbance change, corresponding to approximately three electron equivalents. These three electrons are removed on the first rapid circuit of the catalytic cycle, before flavin re-reduction by glycolate slows turnover dramatically. Once this point has been reached, a steady

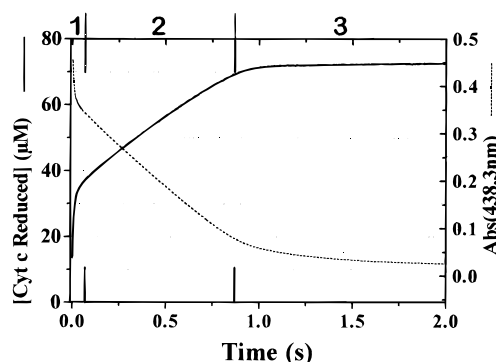


FIGURE 3: Examples of stopped-flow traces generated from a flavin oxidation experiment (see Figure 2) containing 10 μM flavocytochrome *b*₂, 75 μM cytochrome *c*, and 15 mM pyruvate at 25 °C in 10 mM Tris-HCl buffer, pH 7.5, *I* 0.10. The cytochrome *c* trace (left axis) was recorded at the *b*₂-heme isosbestic of 544.8 nm where an absorbance increase is observed as ferricytochrome *c* is reduced. The y-axis for this trace has been converted to concentration of ferrocyanide *c* by using $\Delta\epsilon = 7000$ (see Materials and Methods). This allows the steps described in Figure 2 to be followed in terms of molar equivalents; i.e., since flavocytochrome *b*₂ is present at a concentration of 10 μM (after mixing), each 10 μM ferrocyanide *c* produced represents one molar equivalent. The cytochrome *c* trace is split into three distinct phases; 1, a rapid pre-steady-state phase in which 3 molar equivalents of ferrocyanide *c* are generated; 2, a slow steady-state phase in which turnover is limited by glycolate oxidation; 3, turnover ends when all the cytochrome *c* has been reduced. The trace recorded at the *b*₂-heme isosbestic 438.3 nm (right axis) is almost a mirror image of the cytochrome *c* trace, due to a large negative contribution from cytochrome *c* to the absorbance change at this wavelength. However, there is a significant contribution from the flavin manifested in phase 1, due to flavin oxidation, and phase 3, as flavin reduction occurs. Weighted addition of the two traces to eliminate the common cytochrome *c* contribution leads to the flavin time course illustrated in Figure 4.

state period occurs of approximately 1 s, in which glycolate is oxidized at the expense of cytochrome *c*. Finally, after around 7.5 electron equivalents, all of the cytochrome *c* has been reduced and turnover stops. The ferricytochrome *c* concentration was chosen to be as high as possible to ensure that the first two electron equivalents could be reduced while the flavocytochrome *b*₂ was still saturated. The *K*_m for cytochrome *c* reduction has been measured to be 10 (± 1) μM (Miles et al., 1992), and so even after the first two electron equivalents have been reduced ($\equiv 20 \mu\text{M}$), 55 μM remains, i.e., 5-fold in excess of the *K*_m.

The corresponding flavin trace shows a rapid absorbance increase initially caused by FMN oxidation, a flat period during steady-state, and finally a slow reduction phase once all the cytochrome *c* has been reduced. The amplitude of the FMN contribution to the absorbance change at 438.3 nm was typically around 0.07. This is compatible with the expected change for the semiquinone to oxidized FMN redox change based on previously determined absorption coefficients (Capeillère-Blandin, 1991). The rate constant for the flavin oxidation process was determined to be 120 s⁻¹ by fitting the stopped-flow trace to a single-exponential function. Therefore, although several other steps occur before flavin oxidation they were deemed to be too fast to affect the shape of the trace, and Figure 4 was treated as a single-step reaction. The quality of fit typically achieved by this method suggests that this is a valid assumption. However, one should not ignore the implications of this when considering the error involved in the rate constant. Taking this into account, along with errors generating from the

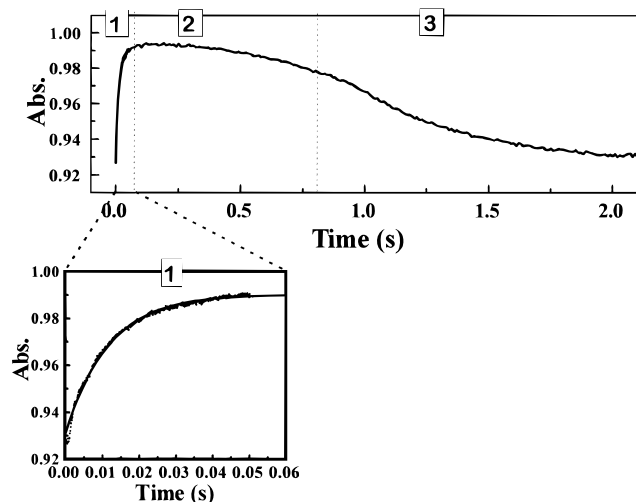


FIGURE 4: Example of a flavin absorbance time course generated by the addition of the stopped-flow traces shown in Figure 3 according to $\text{Abs}(438.3 \text{ nm}) + 1.07\text{Abs}(544.8 \text{ nm})$. The three phases described for Figure 3 are apparent here as follows: 1, flavin oxidation causes an absorbance increase at 438.3 nm; 2, steady-state period during which time the flavin absorbance is approximately constant; 3, flavin reduction which occurs in the presence of excess glycolate once exhaustion of ferricytochrome c has ended the steady-state reaction and returns the absorbance back to its starting point. Phase 1 is shown expanded to illustrate the flavin oxidation process. Although the entire trace contains 1000 data points, the use of split time bases has enabled this small region of the time course to contain 500 data points, allowing it to be accurately fitted to a single-exponential function (as shown).

subtraction of cytochrome c absorbance (see Materials and Methods), the actual rate constant for FMN semiquinone to b_2 -heme electron transfer is estimated to be 120 s^{-1} with an error of 10–20%.

Electron transfer from flavin semiquinone to b_2 -heme has also been studied by laser flash photolysis (Walker & Tollin, 1991), but no electron transfer was observed by this method in the absence of product (pyruvate). Therefore the steps preceding flavin oxidation within the catalytic cycle appear to be critical in determining the rate constant observed.

Pyruvate Inhibition. The flavin oxidation process, seen to occur with rate constant 120 s^{-1} is inhibited by addition of the product pyruvate to the reaction mixture with a K_i of $40 (\pm 17) \text{ mM}$ (Figure 5). These experiments were performed by introducing pyruvate into the ferricytochrome c solution before mixing (see Figure 2). The reason for this was to avoid FMN oxidation by excess pyruvate, although this process is sufficiently slow so as not to compete with the usual catalytic cycle (Urban et al., 1983). Pyruvate is known to be a noncompetitive inhibitor of flavocytochrome b_2 in the steady-state, and the K_i of 30 mM (Lederer, 1978) is consistent with the above result. Conversely, increases in ionic strength or addition of oxalate (a competitive inhibitor) cause the flavin oxidation process to occur more rapidly. However, the single-exponential functions obtained under the initial conditions become more complex, as presumably different steps begin to contribute to rate limitation. This problem is also observed as the rate is slowed down by addition of pyruvate. Contributing factors to the complexity include the effect of increasing ionic strength with increasing pyruvate concentration and also deviation from ideality with respect to pyruvate binding, i.e., the association/dissociation rates may be too slow to create a genuine equilibrium for binding during the pre-steady-state

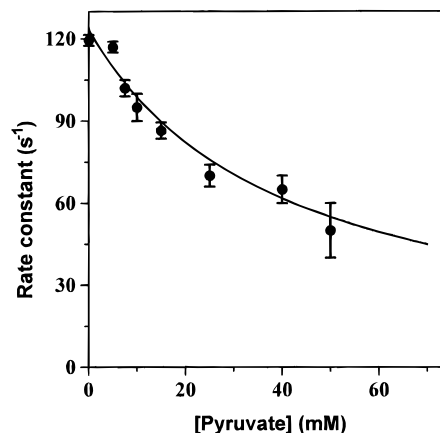


FIGURE 5: Inhibition plot of flavin oxidation rate vs. pyruvate concentration. All experiments were conducted as described in the Materials and Methods, $10 \mu\text{M}$ flavocytochrome b_2 and $75 \mu\text{M}$ cytochrome c (after mixing), in 10 mM Tris-HCl buffer, pH 7.5, I 0.10, at 25°C . Data were fitted to a Michaelis–Menten partial inhibition function using nonlinear least-squares regression analysis. k_0 is the rate constant in the absence of inhibitor, and k_∞ is the minimum rate constant at saturation. This was constrained to >0 during fitting. The error bars represent the range of values collected at each concentration from at least five experiments. $K_i = 40 (\pm 17) \text{ mM}$, $k_0 = 123 (\pm 2) \text{ s}^{-1}$, $k_\infty = 0 (\pm 26) \text{ s}^{-1}$.

reaction. For this reason pyruvate concentrations are limited to less than 50 mM, over which range the data are reliable. However, using such a narrow range limits the accuracy of the K_i derived. For example, it is impossible to say whether the inhibition tends to zero at infinite pyruvate concentrations. Although the accuracy is poor, it is clear that inhibition does occur during this rate-determining electron-transfer step. There are several possibilities for the mechanism of inhibition based on pyruvate binding to the semiquinone form of the enzyme: (1) pyruvate acts as a physical barrier to electron transfer from FMN to b_2 -heme by changing the properties of the intervening medium. (2) Pyruvate stabilizes the semiquinone state thereby altering its redox potential and making electron transfer thermodynamically less favorable [this possibility is discussed in detail by Tegoni et al. (1990) for the related enzyme from *H. anomala* and supported by Walker and Tollin (1991) for the *S. cerevisiae* enzyme]. (3) Pyruvate competes with one of the heme propionates for a key hydrogen bond causing the heme group to be “disconnected” from the active site. This could result in an increase in the flavin–heme separation which would disfavor the electron transfer. Tyr 143 is a suitable candidate for this role in that it is observed to be within hydrogen-bonding distance of both pyruvate and one of the propionates in the enzyme’s crystal structure (Xia & Mathews, 1990). Further, it has been demonstrated that mutation of this residue to phenylalanine greatly disrupts both intramolecular electron transfer and substrate binding (Miles et al., 1992).

Regardless of the mechanism, the fact that pyruvate is able to cause this inhibition suggests that, immediately prior to electron transfer, dissociation of pyruvate has already occurred, and that the active site is vacant. Furthermore, the observation that step 4 (in the absence of pyruvate) occurs at the same rate as in the catalytic cycle suggests that pyruvate dissociation contributes little to the overall rate of turnover.

Quenched-Flow EPR. In order to test the model derived for the catalytic cycle, quenched-flow EPR was used to quantify the amount of flavin semiquinone present when the

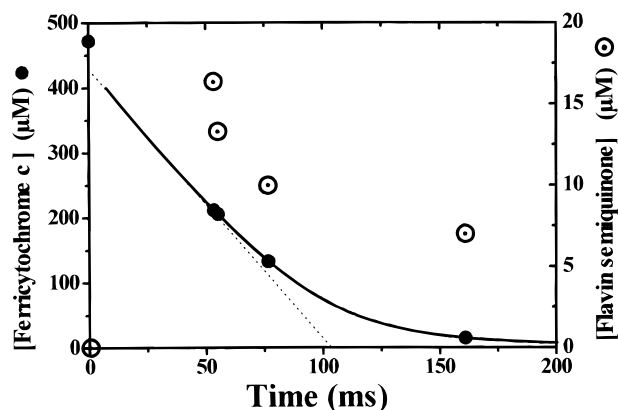


FIGURE 6: Plot of free radical concentrations for both ferricytochrome *c* and flavin semiquinone derived from EPR spectroscopic quantifications of frozen samples of a reaction mixture containing 470 μM cytochrome *c*, 10 mM L-lactate, and 20 μM flavocytochrome *b*₂ mixed at 25 °C in 10 mM MOPS buffer, *I* 0.10, pH 7.5, and freeze-quenched in isopentane liquid at -140 °C. The ferricytochrome *c* quantities have been used to calibrate the time-base for this plot by fixing them to a simulation of the reaction (—), derived by scaling up an assay collected by a visible spectrophotometer with a catalytic amount of flavocytochrome *b*₂. Each of the EPR quantifications have been corrected for the dilution caused by loose packing of the frozen, powdered sample in the EPR tube relative to a standard ferricytochrome *c* sample. Inconsistencies in packing are likely to constitute most of the significant error in the data.

enzyme is turning over at its maximum rate in the presence of saturating amounts of L-lactate (10 mM) and cytochrome *c* (470 μM). Figure 6 plots the concentrations, calculated using EPR spectrometry, of flavin semiquinone and ferricytochrome *c* in each frozen sample relative to the reaction time base. The ferricytochrome *c* quantifications provide an internal indication of the extent of the reaction and therefore allow the semiquinone concentration values to be fixed to their correct positions along the time axis. This calibration was performed using a spectrophotometrically collected trace identical to the above reaction, but using only a catalytic amount of flavocytochrome *b*₂, which was then scaled up to provide an approximate simulation of the quenched-flow experiment. Although the free radical concentrations are imprecise, due mainly to the problem of achieving uniform sample packing within the EPR tube, the data show that after 50 ms, during the rapid turnover period, around 75% of the total enzyme present is in the semiquinone form. This result is entirely compatible with the kinetic model derived.

CONCLUSIONS

Many of the steps within the catalytic cycle of flavocytochrome *b*₂ have been studied before, but the intramolecular electron transfer between FMN semiquinone and *b*₂-heme has proved difficult to observe. In this paper we demonstrate a method for achieving this which is of particular relevance to the catalytic cycle, by observing the rate of FMN oxidation by ferricytochrome *c* using stopped-flow spectrophotometry. The rate constant obtained for the electron transfer is 120 s^{-1} , which appears to rate-limit the overall catalytic cycle to 100 s^{-1} . Confirmation of this comes from quenched-flow EPR experiments which show that, during steady-state turnover, around 75% of the enzyme is in the FMN semiquinone form. We also show that FMN oxidation is inhibited by pyruvate binding. The inhibition constant obtained ($K_i = 40 (\pm 17)$ mM) is consistent with the steady-state value for noncompetitive inhibition.

The reason why FMN semiquinone to *b*₂-heme electron transfer is so slow in comparison to that from FMN hydroquinone to *b*₂-heme ($> 1500 \text{ s}^{-1}$) is unclear. Based on electrode potentials for the redox couples involved in the two one-electron transfers, one would expect semiquinone to heme electron transfer to be faster than that for hydroquinone to heme (Walker & Tollin, 1991). The scope for conformational influences on electron-transfer rate constants is extensive in this case owing to the significant mobility of the two prosthetic groups with respect to each other. Such factors mean that the electron-transfer rate constants are likely to be altogether less predictable than for systems in which electron-transfer distance and prosthetic group orientation are fixed. Evidence for the mobility of the *b*₂-heme domain is derived from crystallographic (Xia & Mathews, 1990) and NMR data (Labeyrie et al., 1988), while the significance of the interdomain hinge region has been studied by mutagenesis (Sharp et al., 1994; White et al., 1993).

REFERENCES

- Balme, A., Brunt, C. E., Pallister, R. L., Chapman, S. K., & Reid, G. A. (1995) *Biochem. J.* 309, 601–605.
- Black, M. T., White, S. A., Reid, G. A., & Chapman, S. K. (1989) *Biochem. J.* 258, 255–259.
- Capeillère-Blandin, C. (1975) *Eur. J. Biochem.* 56, 91–101.
- Capeillère-Blandin, C. (1991) *Biochem. J.* 274, 207.
- Capeillère-Blandin, C., Bray, R. C., Iwatsubo, M., & Labeyrie, F. (1975) *Eur. J. Biochem.* 54, 549–566.
- Chapman, S. K., Reid, G. A., Daff, S., Sharp, R. E., White, P., Manson, F. D. C., & Lederer, F. (1994) *Biochem. Soc. Trans.* 22, 713–718.
- Daff, S., Sharp, R. E., Short, D. M., Bell, C., White, P., Manson, F. D. C., Reid, G. A., & Chapman, S. K. (1996) *Biochemistry* 35, 6351–6357.
- Daum, G., Böhm, P. C., & Schatz, G. (1982) *J. Biol. Chem.* 257, 13028–13033.
- Forestier, J.-P., & Baudras, A. (1971) in *Flavins & Flavoproteins* (Kamin, H., Ed.) pp 599–605, University Park Press, Baltimore, MD.
- Hazzard, J. T., McDonough, C. A., & Tollin, G. (1994) *Biochemistry* 33, 13445–13454.
- Iwatsubo, M., Mével-Ninio, M., & Labeyrie, F. (1977) *Biochemistry* 16, 3558–3566.
- Janot, J.-M., Capeillère-Blandin, C., & Labeyrie, F. (1990) *Biochim. Biophys. Acta* 1016, 165–176.
- Labeyrie, F., Beloeil, J. C., & Thomas, M. A. (1988) *Biochim. Biophys. Acta* 953, 134–141.
- Lederer, F. (1978) *Eur. J. Biochem.* 88, 425–431.
- Miles, C. S., Rouviere-Fourmy, N., Lederer, F., Mathews, F. S., Reid, G. A., & Chapman, S. K. (1992) *Biochem. J.* 285, 187–192.
- Moodie, A., Mitchell, R., & Ingledew, W. J. (1990) *Anal. Biochem.* 189, 103–106.
- Pajot, P., & Groudinsky, O. (1970) *Eur. J. Biochem.* 12, 158–164.
- Pompon, D. (1980) *Eur. J. Biochem.* 106, 151–159.
- Pompon, D., Iwatsubo, M., & Lederer, F. (1980) *Eur. J. Biochem.* 104, 479–488.
- Sharp, R. E., White, P., Chapman, S. K., & Reid, G. A. (1994) *Biochemistry* 33, 5115–5120.
- Tegoni, M., Janot, J.-M., & Labeyrie, F. (1986) *Eur. J. Biochem.* 155, 491–503.
- Tegoni, M., Janot, J.-M., & Labeyrie, F. (1990) *Eur. J. Biochem.* 190, 329–342.
- Urban, P., Alliel, P. M., & Lederer, F. (1983) *Eur. J. Biochem.* 134, 275–281.
- Walker, M. C., & Tollin, G. (1991) *Biochemistry* 30, 5546–5555.
- White, P., Manson, F. D. C., Brunt, C. E., Chapman, S. K., & Reid, G. A. (1993) *Biochem. J.* 291, 89–94.
- Xia, Z.-X., & Mathews, F. S. (1990) *J. Mol. Biol.* 212, 837–863.